ResearchGate

See discussions, stats, and author profiles for this publication at: https://www.researchgate.net/publication/225183350

Subscriber Synthesis of Different Cu(OH) 2 and CuO (Nanowires, Rectangles, Seed-, Belt-, and Sheetlike) Nanostructures by Simple Wet Chemical Route More About This Article Synthesi...

ARTICLE *in* THE JOURNAL OF PHYSICAL CHEMISTRY C · MARCH 2009

Impact Factor: 4.77 · DOI: 10.1021/jp804832g

CITATIONS
90

READS
1,509

3 AUTHORS, INCLUDING:

Dinesh PRATAP Singh
University of Santiago, Chile
41 PUBLICATIONS **592** CITATIONS

SEE PROFILE

Available from: Dinesh PRATAP Singh
Retrieved on: 01 February 2016

THE JOURNAL OF PHYSICAL CHEMISTRY C

Subscriber access provided by Southern Illinois University | Morris Library

Article

Synthesis of Different Cu(OH) and CuO (Nanowires, Rectangles, Seed-, Belt-, and Sheetlike) Nanostructures by Simple Wet Chemical Route

Dinesh Pratap Singh, Animesh Kumar Ojha, and Onkar Nath Srivastava

J. Phys. Chem. C, **2009**, 113 (9), 3409-3418• DOI: 10.1021/jp804832g • Publication Date (Web): 06 February 2009

Downloaded from http://pubs.acs.org on March 9, 2009

More About This Article

Additional resources and features associated with this article are available within the HTML version:

- Supporting Information
- Access to high resolution figures
- Links to articles and content related to this article
- Copyright permission to reproduce figures and/or text from this article

View the Full Text HTML

ACS Publications
High quality. High impact.

The Journal of Physical Chemistry C is published by the American Chemical Society. 1155 Sixteenth Street N.W., Washington, DC 20036

Synthesis of Different $Cu(OH)_2$ and CuO (Nanowires, Rectangles, Seed-, Belt-, and Sheetlike) Nanostructures by Simple Wet Chemical Route

Dinesh Pratap Singh,*,† Animesh Kumar Ojha,‡ and Onkar Nath Srivastava†

Department of Physics, Banaras Hindu University, Varanasi 221005, India, and Department of Physics, Motilal Nehru National Institute of Technology, Allahabad 211004, India

Received: June 1, 2008; Revised Manuscript Received: December 26, 2008

We report the synthesis of different $Cu(OH)_2$ and CuO nanostructures (nanowires, rectangles, seedlike, beltlike, and sheetlike) in a solution phase with high yield at low cost by simple reduction of aqueous solution of copper nitrate ($Cu(NO_3)_2 = 0.2$ M) with different alkaline solutions of sodium hydroxide (NaOH = 0.1, 0.25, 0.50, 0.75, and 1.0 M). The morphology of the synthesized nanostructures is significantly influenced by the feeding concentration of alkaline NaOH solution. $Cu(OH)_2$ rectangles and nanowires can be readily obtained by the reduction of $Cu(NO_3)_2$ solution with different molar concentrations of NaOH solution and the synthesized nanomaterials get transformed into different nanostructures of CuO by subsequent heat treatment at 80 °C for half an hour. Well-defined rectangle-like structures of hydrated copper hydroxide $Cu(OH)_2 \cdot H_2O$ and different CuO nanostructures, such as seedlike, beltlike, and sheetlike, were synthesized by thermal dehydration of corresponding different shaped and sized $Cu(OH)_2$ nanomaterials. The Raman spectra of different CuO nanomaterials obtained at different molar concentrations of NaOH (0.25, 0.50, 0.75, and 1 M) were recorded in the region 1050−1300 cm^{-1}. A tentative mechanism has been given for the formation and transformation of different nanostructures.

1. Introduction

Synthesis of inorganic nanostructures at reliable low cost and well-defined morphology has attracted considerable attention for the dimensional and structural characteristics of these materials endowed with a wide range of potential applications in electronic magnetic and photonic devices. The unique properties of semiconductor and metal oxides could be harnessed for the design and fabrication of nanosensors,[1] switches,[2] nanolasers,[3] and transistors.[4] Among different metal oxide materials, copper-based nanomaterials (nanowires and nanobelts, etc.) are of great interest because of their applications as interconnects for microelectronics. Copper-containing complexes are indispensable in biological processes for their ability to act as oxygen carriers in oxidation reactions[5] involving DNA hydroxocomplexes[6] and in biological enzymes such astyrosinase[7] and oxyhemocyanin.[8] Orthorhombic copper hydroxide, $Cu(OH)_2$, is a well-known copper-based layered material. The magnetic properties of $Cu(OH)_2$ are remarkably sensitive to the intercalation of molecular anions,[9−11] making the material a candidate for the sensor applications. $Cu(OH)_2$ nanowires have been thought to be the precursors for the synthesis of Cu_2O nanowires.[12] It has been long known that these materials tend to give needle-type crystals in water.[13−15] Long and narrow fibers with a width of 20−100 nm were obtained by Yang et al. through the conversion of Cu_2S nanowires into $Cu(OH)_2$ in an aqueous solution of ammonia.[16] Similar crystalline nanofibers were obtainable by directly treating the surface of a copper foil with an alkaline solution.[17] Recently, aligned nanorods of $Cu(OH)_2$ were synthesized from two-dimensional $Cu_2(OH)_3NO_3$, a basic copper salt, by anion exchange using sodium hydroxide.[18] Preparation of narrow $Cu(OH)_2$ nanofibers has been reported by a few research groups.[19−21] Specifically, Song and co-workers reported that extremely narrow nanofibers of 4−5 nm in diameter were observed in their fibrous materials.[21] Extremely narrow positively charged $Cu(OH)_2$ nanostrands with a diameter of 2.5 nm were prepared by Luo et al.[22]

As an important p-type transition metal oxide with a band gap ($E_g = 1.2$ eV), CuO forms the basis of several high-temperature superconductors and giant magnetoresistance materials.[23,24] It is also a promising material for fabricating solar cells,[25,26] owing to its photoconductive and photochemical properties, and lithium ion batteries.[27,28] CuO has also been widely exploited for application such as powerful heterogeneous catalyst (to convert hydrocarbons completely into carbon dioxide and water),[29] magnetic storage media, and gas sensors.[30−32] Monoclinic CuO solid belongs to a particular class of materials known as Mott insulators, whose electronic structures cannot be simply described by conventional band theory.[33,34] Recent studies indicate that CuO could exist in as many as three different magnetic phases.[35,36] It is a 3D collinear antiferromagnet at temperatures below 213 K. When the temperature is raised, it first becomes an intermediate noncollinear incommensurate magnetic phase up to 230 K and then acts like a 1D quantum antiferromagnetic material. Well-defined CuO nanostructures with different dimensionalities such as nanoparticles nanoneedles, nanowires, nanowhiskers, nanoshuttles, nanoleaves, nanorods, nanotubes, nanoribbons,[37−44] 3D peanut-like patterns,[45] pricky/layered microspheres,[46,47] nanodendrites,[48] nanoellipsoids,[49] dandelion-shaped hollow structures, [50] and chrysanthemum-like architectures[51] have been obtained by solution-based routes; vapor-phase processes, thermal decomposition, water baths, hydrothermal methods, natural oxidation process require relatively high temperature, complicated procedures, expensive equipments, and long reaction times. The wet chemical method has been considered to be one of the most

* Corresponding author. E-mail: dineshbhu@gmail.com, dpsinghbhu@gmail.com. Phone: +919415813214. Fax: +915422307307.
† Banaras Hindu University.
‡ Motilal Nehru National Institute of Technology.

10.1021/jp804832g CCC: $40.75 © 2009 American Chemical Society
Published on Web 02/06/2009

promising synthetic routes, due to its low cost, its high yield, and its good potential for high-quality production. Generally, it can be classified into two kinds: the template methods which employ hard templates (AAO, silicon wafers, metallic foils) and soft templates (surfactant and capping agents) and the template-free method. However, the introduction of templates into the synthetic routes is still troublesome and sometimes difficult to handle. Therefore, developing simple methods without using templates or other additives seems to be more promising because of the various expected advantages.

In the present work, we report a template-free wet chemical approach for the synthesis of copper hydroxide nanomaterials and their subsequent transformation in to cupric oxide (CuO) nanostructures by heat treatment. The method is very simple, with low cost and high yield and a specialty that different nanostructures can be synthesized by a simple variation in concentration of alkaline solution sodium hydroxide (NaOH).

2. Experimental Section

2.1. Synthesis of $Cu(OH)_2$ Nanomaterials. The present method makes use of a 0.2 M copper nitrate [$Cu(NO_3)_2$] solution with a varied feeding concentration of alkaline NaOH solution. Different concentrated solutions of NaOH were added drop by drop in $Cu(NO_3)_2$ solution under magnetic stirring condition at room temperature. Both the solutions were mixed in a ratio of 1:1 (50 mL each) and the concentration of NaOH was varied as 0.1, 0.25, 0.50, 0.75, and 1 M in different experiments. As soon as the NaOH solution is mixed into the $Cu(NO_3)_2$ solution the whole solution turned into light blue or blue color precipitate. The obtained materials were washed with distilled water and dried for the characterization through different techniques.

2.2. Transformation of $Cu(OH)_2$ to CuO Nanostructures. In other experiments, the as-obtained blue color materials after adding different concentrations of NaOH solution to the $Cu(NO_3)_2$ solution were heated 80 °C for half an hour in every case. Heating of the materials helped in better crystallization of materials and in the formation of different nanostructures of CuO. Gradually the blue color materials as obtained at different concentration of NaOH turned into gray and black color, except at the concentration of 0.1 M NaOH, which remained in the form of light blue color. The as-obtained materials were washed with deionized water several times and dried at ambient condition. The black color precipitate is a feasible indication of the formation of copper oxide nanomaterials. The as-obtained materials were further characterized by XRD, TEM, and SEM.

2.3. Structural/Microstructural Characterization. The as-synthesized materials were characterized by X-ray diffractometer (XRD), scanning electron microscopy (SEM), and transmission electron microscopy (TEM). XRD was carried out on a diffractometer X-Pert PRO PANalytical with Cu Kα radiation (λ = 1.5418 Å), operating at 30 kV and 20 mA. TEM was performed on a Philips EM, CM-12 and Technai $20G^2$ microscope with an accelerating voltage of 120 and 200 kV, respectively. SEM images were taken with a Philips XL-20 operated at 30 kV. The Raman spectra of different CuO samples were recorded in the region 1050−1300 cm^{-1}. The spectra were measured in backscattering geometry using a 488 nm argon ion laser as an excitation source. The spectrometer was equipped with a 1200 grooves/mm holographic grating, a holographic supernotch filter, and a Peltier-cooled CCD detector.

3. Results and Discussion

3.1. Characterization of $Cu(OH)_2$ Nanomaterials. Figure 1a shows the XRD pattern of as-obtained samples after the mixing of 0.2 M $Cu(NO_3)_2$ solution with the different molar NaOH solutions. All the peaks can be indexed to the orthorhombic $Cu(OH)_2$ in good agreement with JCPDS No (35-0505). Broadening in the peaks of $Cu(OH)_2$ crystals indicate the formation of $Cu(OH)_2$ nanostructures. The light blue or blue color precipitate was observed in every case of the experiment when the $Cu(NO_3)_2$ solution was added with different molar concentrations of NaOH solution. After precipitation the precipitates were washed with several times with distilled water. The resultant blue color precipitate was filtered off and dried. Panels b−f of Figure 1 are the SEM micrographs of as-obtained different $Cu(OH)_2$ nanomaterials at different alkaline solution of NaOH (0.1, 0.25, 0.50, 0.75, and 1 M). In each micrograph the molar concentration of NaOH is indicated in the inset.

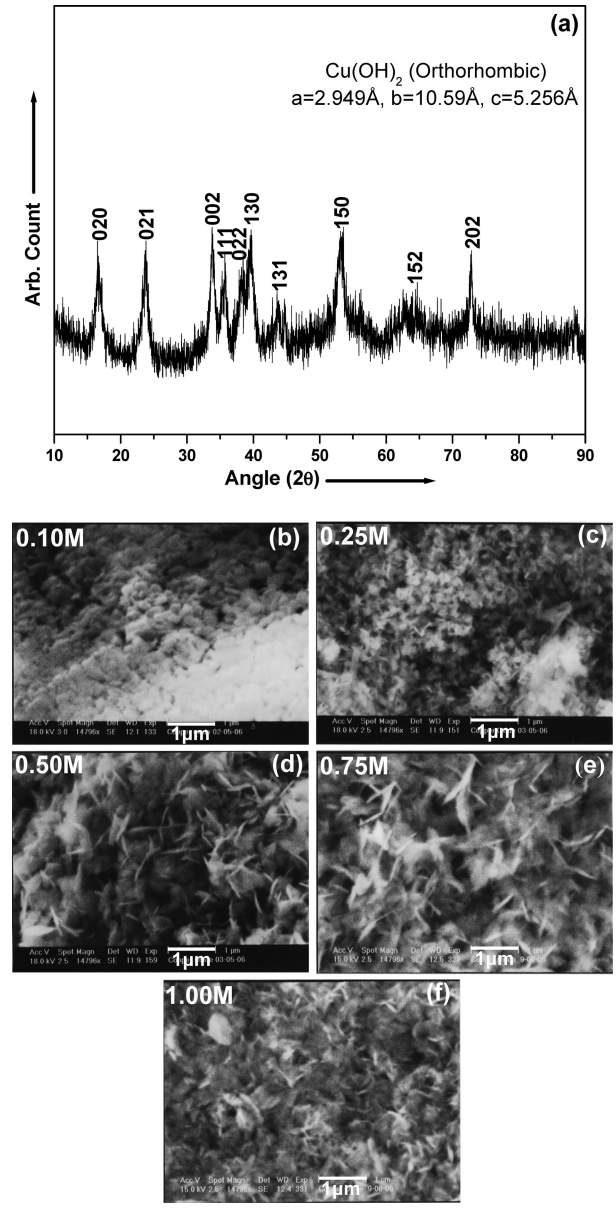

Figure 1. (a) XRD pattern of the copper hydroxide nanostructures obtained after addition of NaOH solution to the copper nitrate solution (0.2 M). (b−f) SEM micrographs of the copper hydroxide ($Cu(OH)_2$) nanomaterials after addition of varied molar concentration of NaOH solution (0.1, 0.25, 0.50, 0.75, and 1M) to the copper nitrate solution (0.2M) in ratio 1:1 (without annealing).

The panels a−o of Figure 2 are the TEM micrographs of the as-obtained blue color precipitate of $Cu(OH)_2$ nanomaterials. The molar concentrations of reducing NaOH are indicated in

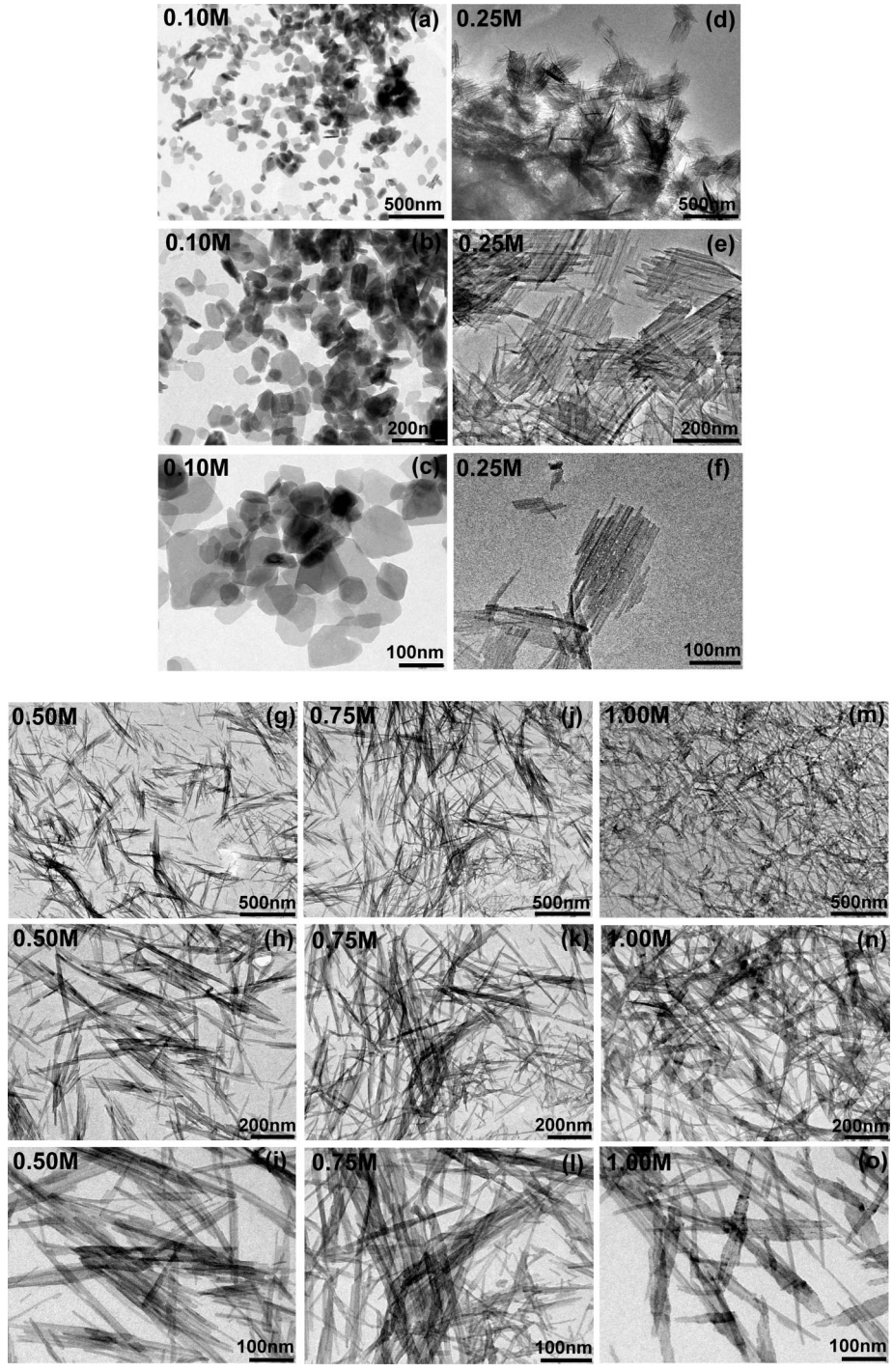

Figure 2. (a−c) TEM micrographs of the rectangle shaped ($Cu(OH)_2$) nanomaterials after addition of 0.10 M NaOH solution to the copper nitrate solution. (d−f) TEM micrographs of the $Cu(OH)_2$ nanomaterials after addition of 0.25 M NaOH solution. It can be seen that the fine nanowires of $Cu(OH)_2$ are assembling in ellipsoid manner. (g−i) TEM micrographs of the $Cu(OH)_2$ nanomaterials, obtained after addition of 0.50 M NaOH solution. (j−l) TEM micrographs of the $Cu(OH)_2$ nanomaterials after addition of 0.75 M NaOH. (m−o) TEM micrographs of the $Cu(OH)_2$ nanomaterials after addition of 1.00 M NaOH solution.

the inset of the panels. Panels a−c of Figure 2 are the TEM micrographs of the light blue color precipitate as obtained after reduction of $Cu(NO_3)_2$ solution with 0.1 M solution of NaOH. The micrographs revealed the formation of rectangle or irregular shaped nanoparticles. The size of the nanoparticles ranges between 20 and 125 nm.

As we have increased the molar concentration of NaOH to 0.25 M, a large number of fine nanowires of $Cu(OH)_2$ are observed in the TEM micrographs. Panels d−f of Figure 2 are the TEM micrographs at different magnifications of the as-obtained materials after reduction with 0.25 M solution of NaOH. The TEM micrographs revealed the formation of fine nanowires of diameter 5−10 nm and length 20−200 nm. An interesting observation from TEM micrographs is that these nanowires have a high tendency to arrange in a special manner. Figure 2f is a TEM micrograph of an isolated such assembled nanowire in ellipsoid manner. It can be clearly observed from the TEM micrographs of Figure 2d−f that first the fine nanowires of $Cu(OH)_2$ are formed and these nanowires have a very high tendency to assemble in a typical manner of ellipsoid shape and resulted in the morphology as shown in Figure 2f.

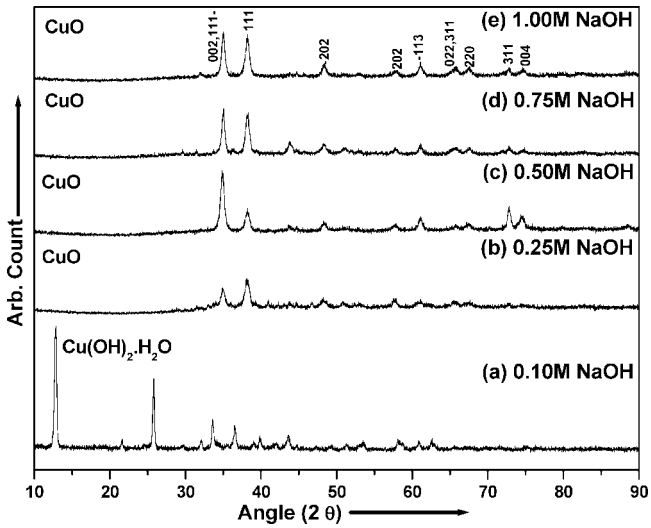

Figure 3. XRD patterns of (a) the hydrated copper hydroxide at 0.1 M NaOH and (b−e) different nanostructures of copper oxide after addition of varied molar concentrations of NaOH solution (0.25, 0.50, 0.75, and 1 M) to the copper nitrate solution (0.2 M) in ratio 1:1 and followed by annealing at 80 °C for half an hour in each case.

Panels g−i of Figure 2 are the TEM micrographs of the as-obtained materials after reduction with 0.50 M solution of NaOH. The micrographs revealed the formation of fine nanowires of long length ∼500 nm and diameter ∼10 nm. These nanowires have also the tendency to assemble in parallel to their length. As we have further increased the molar concentration to 0.75 M NaOH, nearly the same morphology has been observed. The only difference is that in this case the nanowires are of longer size ∼500 nm and have poor tendency to assemble as shown in Figure 2j−l.

Panels m−o of Figure 2 are the TEM micrographs of the as-obtained materials after reduction with 1.00 M solution of NaOH. The micrographs revealed the formation of longer size nanowires ∼500 nm and these nanowires have a tendency to assemble in ellipsoid manner as previously observed in the case of 0.25 M NaOH. Figure 2o is the magnified TEM micrograph of several nanostructures of such morphology.

3.2. Characterization of $Cu(OH)_2.H_2O$ and CuO Nanostructures. To see the effect of temperature on the various synthesized nanostructures of $Cu(OH)_2$, the as-obtained materials at different molar concentrations of NaOH solution were further heated at 80 °C for half an hour in every case. The obtained materials after drying in ambient condition were characterized by XRD, SEM, and TEM for structural/microstructural characterization. Figure 3 is X-ray diffraction pattern of the different samples obtained after heating the materials at 80 °C for half an hour. Figure 3, a−e, shows the XRD pattern at different alkaline concentration of 0.1, 0.25, 0.50, 0.75, and 1 M, respectively. XRD patterns Figures 1a and 3 revealed that as we add the copper nitrate solution to the NaOH solution, instantaneously $Cu(OH)_2$ nanostructures get formed and the subsequent heat treatment transformed them into hydrated copper hydroxide $Cu(OH)_2 \cdot H_2O$ and cupric oxide nanostructures at different concentration. Figure 3a illustrates the formation of highly crystalline hydrated copper hydroxide nanostructures. All peaks could be indexed to hydrated copper hydroxide JCPDF No (42-0638), though there are also some peaks of cuprous oxide. The color of these synthesized materials was light blue. All the XRD peaks of the materials shown in Figure 3b−e could be indexed to copper oxide, CuO, and they were black in color. Broadening in the peaks revealed the formation of nanocrystalline copper oxide. In the case of 0.25 M the growth has occurred in the direction of 111, i.e., 111 peak is more intense than the $\bar{1}11$ peak whereas in the case of 0.50, 0.75, and 1 M, the $\bar{1}11$ peak is more intense than the 111 and therefore in these cases the growths are more favorable in the $\bar{1}11$ direction than 111 direction. Intensity of the XRD peaks in the 0.50, 0.75, and 1 M cases is much more than the intensity of the peaks in the case of 0.25 M NaOH, which reveals that the nanostructures of cupric oxide obtained at higher concentration of NaOH are higher crystalline in nature also. Further TEM observation also reinforced the XRD observation.

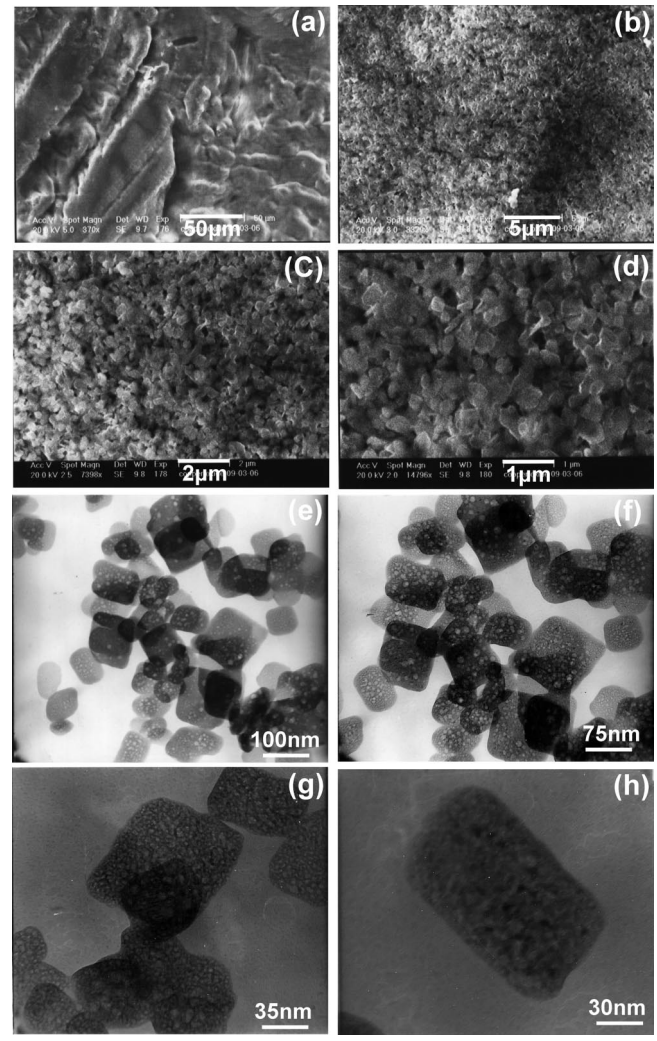

Figure 4. SEM image (a−d) and TEM micrographs (e−h) of rectangle-like nanostructures of hydrated copper hydroxide $Cu(OH)_2 \cdot H_2O$ as synthesized after addition of 0.1 M concentration of NaOH solution to the copper nitrate solution followed by annealing at 80 °C for half an hour.

Figure 4a−d shows the SEM micrographs of light blue color precipitate as obtained after annealing of addition of 0.1 M concentrated NaOH solution to copper nitrate solution. Figure 4a,b reveals the image of the materials at lower and higher magnification. The images reveal the small rectangle- and square-like particles in the materials of size ∼50−200 nm. Figure 4e,f shows the TEM micrographs of these materials. TEM microstructures revealed the rectangle-like particles of varied size ranges 50−100 nm. It has been already seen from the XRD of Figure 3b that these structures are of hydrated copper hydroxide. These new structures of hydrated copper hydroxide are in controlled growth at particular concentration

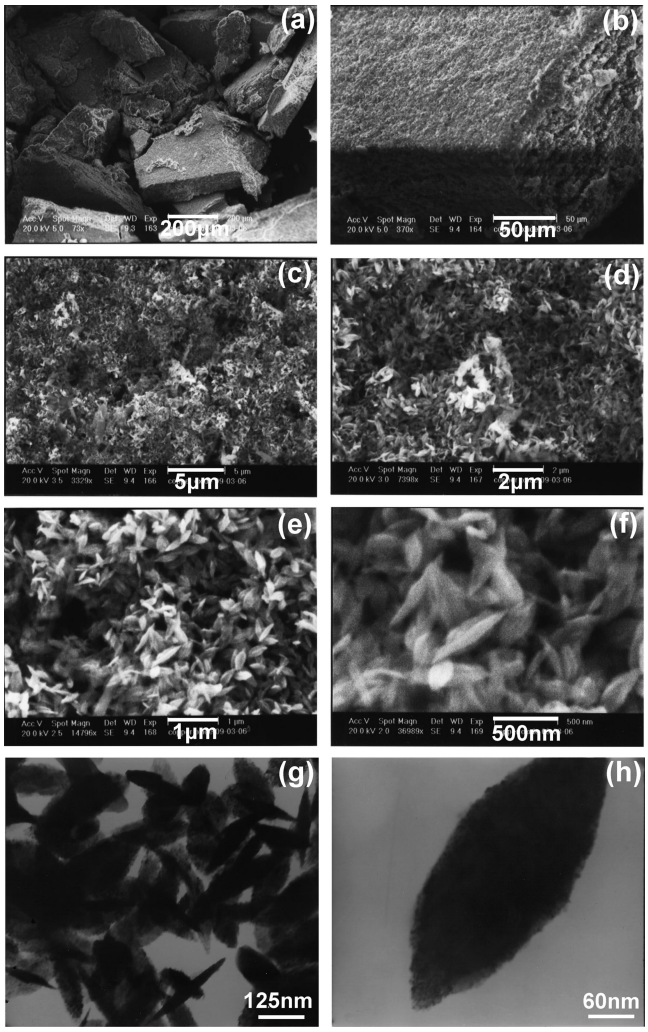

Figure 5. SEM image (a−f) and TEM micrographs (g, h) of seedlike nanostructures of copper oxide as synthesized after addition of 0.25 M concentration of NaOH solution to the copper nitrate solution followed by annealing at 80 °C for half an hour.

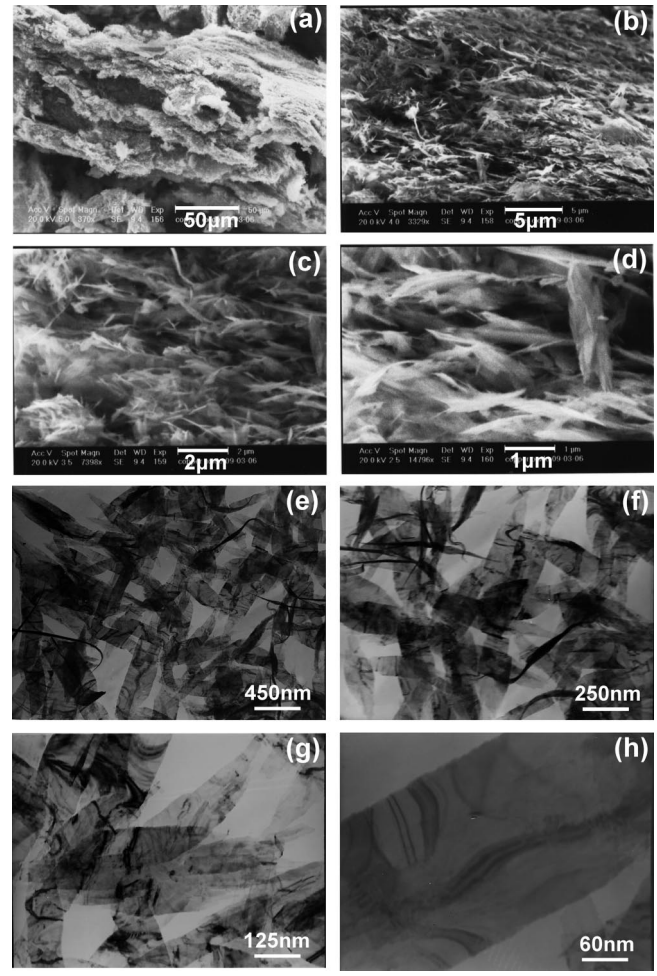

Figure 6. SEM image (a−d) and TEM micrographs (e−h) of beltlike nanostructures of copper oxide as synthesized after addition of 0.50 M NaOH solution to the copper nitrate solution followed by annealing at 80 °C for half an hour.

and temperature and may reveal new electronic and optical properties. These structures were highly reactive to electron beam and as soon as the electron beam was incident on it, the structures got readily damaged. The rectangle-like particles transformed into small porous structures inside it, which can be clearly seen in Figure 4, g and h. Figure 4h is a TEM micrograph of single rectangle-like particle of length 100 nm and width 50 nm. This particle is associated with a large number of small pores inside it. Actually, pores do not exist originally in the structure. As soon as the electron beam is incident on the hydrated copper hydroxide material the dehydration takes place. We think due to this electron beam heating and dehydration of structures the corresponding pores are created.

As we increased the alkaline concentration to 0.25 M NaOH the gray color precipitate was observed. As XRD pattern revealed already that this precipitate is of the CuO. Panels a−f of Figure 5 are the SEM micrographs of the as-obtained annealed material after addition of 0.25 M NaOH solution to the copper nitrate solution. Figure 5a is the SEM micrograph which reveals the slablike materials synthesized in large quantity. The surface of the slab was successively magnified and Figure 5b−f is the magnified SEM micrographs of a slab. Figures 5, e and f, reveals the seedlike nanostructures in a homogeneous manner at the surface of the slab. The figures indicate that these slabs are made up of seedlike nanostructures. Figure 5g,h is the TEM micrographs of the same material which is also a clear evidence of seedlike nanostructures of size 300−500 nm.

Figures 6a−d are the SEM micrographs of as obtained annealed materials after addition of 0.50 M NaOH solution to the copper nitrate solution. Figure 6a,b is the magnified and panels c and d are the higher magnified SEM micrographs revealing that these material are made up of elongated beltlike nanostructures. Figure 6e,h shows the TEM micrographs that revealed the same beltlike nanostructures. These structures are highly crystalline and were not opaque to electron beam. These structures were transparent to electron beam. The length of the belt is up to several micrometers and width 100−125 nm.

Panels a−d of Figure 7 are the SEM micrographs of annealed materials as obtained after addition of 0.75 M NaOH solution to copper nitrate solution. Panels a−d of Figure 7 are the evidence of sheetlike nanostructures of length up to several micrometers. These sheetlike structures are of CuO and highly crystalline in nature as previously observed in XRD of Figure 3e. Panels e−g of Figure 7 are the TEM micrographs of these sheetlike nanostructures showing the width ∼200 nm. Contrast contour in the TEM micrographs of Figure 7e,g shows the high crystallinity of the sheetlike nanostructures.

Figures 8a−d are the low and high magnified SEM micrographs of annealed materials as obtained after addition of 1 M concentration of NaOH solution to the copper nitrate solution.

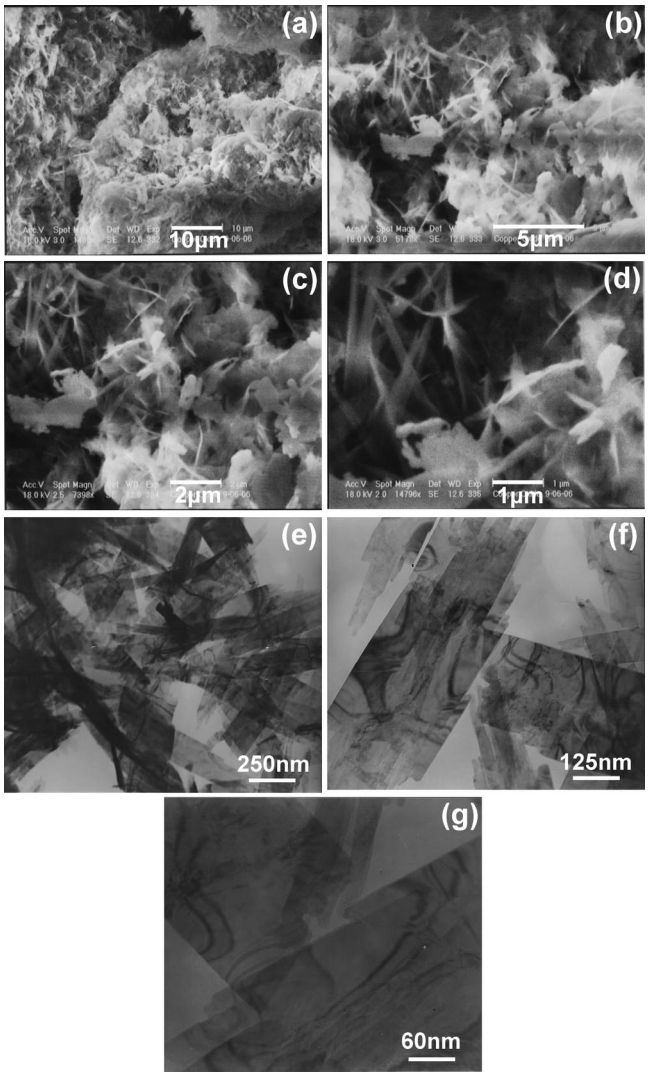

Figure 7. SEM images (a−d) and TEM micrographs (e−g) of sheetlike nanostructures of copper oxide as synthesized after addition of 0.75 M NaOH solution to the copper nitrate solution followed by annealing at 80 °C for half an hour.

TEM micrographs shown in Figure 8e,f show that these structures are highly crystalline in nature and having the shapes seedlike as well as sheetlike. XRD pattern has already revealed that in this type of structure the growth has occurred in same way in both the directions $\bar{1}11$ and 111, as the intensities of the both peaks are near about same. The microstructures shown in Figure 8d−f revealed that the structures are crystalline as sheetlike and shape as seedlike nanostructures. The lengths of these structures are 700−1000 nm and have varied widths of ∼50 nm at the edge and ∼150 nm in the middle portion of the structures.

3.3. Raman Spectroscopic Characterization of Different CuO Nanostructures. The Raman spectra of CuO nanostructures of various shapes and sizes at different molar concentrations of NaOH (NaOH = 0.25, 0.50, 0.75, and 1.0 M) were recorded in the region 1050−1300 cm^{-1}. The spectra were measured in backscattering geometry using a 488 nm argon ion laser as excitation source. The spectrometer was equipped with a 1200 grooves/mm holographic grating, a holographic supernotch filter, and a Peltier-cooled CCD detector. The data acquisition time for each spectrum was 120 s. The expected spectral resolution was around 0.5 cm^{-1} in the present setup. The experimentally recorded spectra as well as fitted spectra in

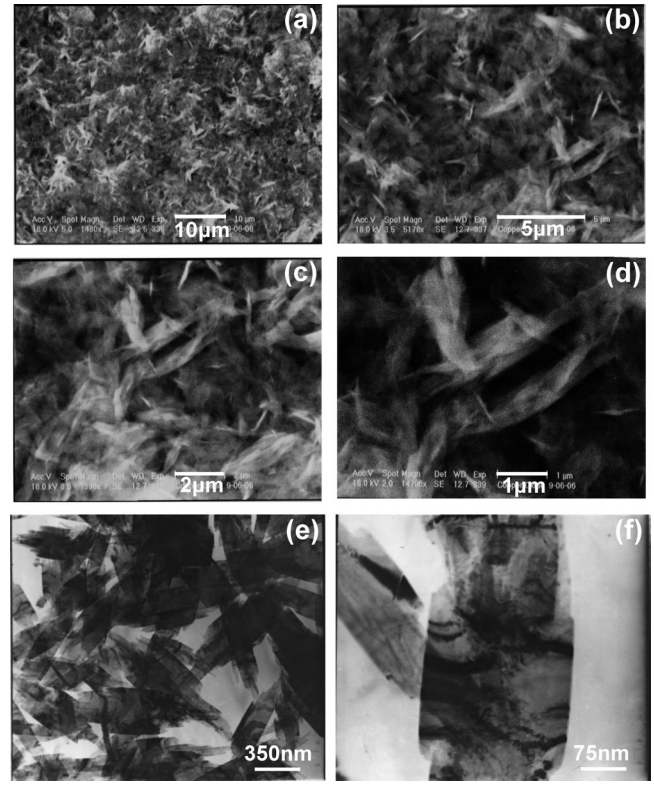

Figure 8. SEM image (a−d) and TEM micrographs (e,f) of seed mediated sheetlike nanostructures of copper oxide as synthesized after addition of 1 M NaOH solution to the copper nitrate solution followed by annealing at 80 °C for half an hour.

the region 1050−1300 cm^{-1} at different molar solutions of NaOH are shown in Figure 9. All the spectra in Figure 9 have one broadened feature ∼1158 cm^{-1}. In order to get the exact values of spectral parameters like Raman shift, line width, and intensity at each molar concentration, a rigorous line-shape analysis was carried out. A nonlinear fitting was made for all the spectra with standard software Spectra-Calc. The curve fitting was made considering the band as mixture of Lorentzian and Gaussian, which is essentially as good as Voigt profile. To check the uniqueness of the fitting results, each spectrum was fitted with different reasonable initial guesses and each time we obtained the same fitting profile and fitting parameters.

The nonlinear fits of the spectra of samples 0.25, 0.50, 0.75, and 1.0 M exhibit a single band at ∼1158, 1158, 1160, and 1158 cm^{-1}, respectively. These peaks belong to B_g symmetry species and arise due to the multiphonon (MP) transition. The spectral parameters such as peak position, line width, and intensity obtained after fitting the spectra are presented in the table in Figure 9. A closer examination of the data presented in the table shows that the multiphonon peak at 0.25 M concentration exhibits blue shift than that at 1 M concentration. The blue shift of the Raman band would be explained in terms of slight lattice contraction, which is proved by the XRD data. The line width of the MP band in 0.25, 0.50, and 0.75 M concentration is the same; however, the MP peak in 0.25 M concentration shows narrowing and the MP peak in 1.00 M concentration shows broadening in the line profile. With this observation, one can conclude that the lifetime of phonon in the former case is larger compared to that in the latter case. The change in phonon lifetime is basically caused due to the different shape and size morphology of the nanostructures. The intensity of the MP band is different at all the concentrations. As per our understanding, the multiphonon band arises due to the anhormonic coupling

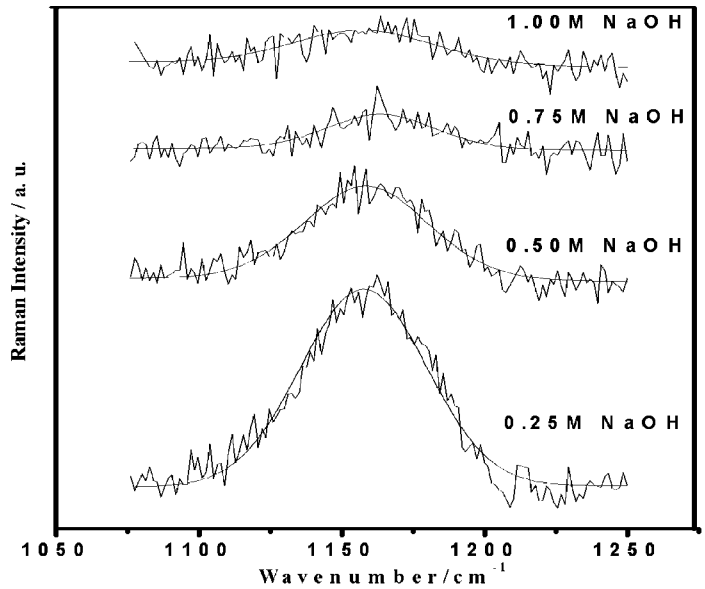

Sample		Peak Position (cm^{-1})	Intensity	Linewidth (cm^{-1})
1	0.25M	1158	61	53
2	0.50M	1158	128	53
4	0.75M	1160	21	53
6	1.00M	1158	22	60

Figure 9. Recorded Raman spectra of different CuO nanostructures obtained at 0.25, 0.50, 0.75, and 1 M NaOH solution.

between phonons in polar solid and its intensity is much more less than that of the one-phonon band, since Raman intensity is related to the electron−phonon interaction. The variation in the intensity shows a finite size and crystallinity effect of CuO nanostructures. The intensity of MP band may also be enhanced due to the electronic movement along the $x-y$ plane by the photoexcitation, which may exist in the anisotropic CuO nanowires. In the present study, the shapes of the CuO nanostructures are close to ellipsoid and therefore the anisotropic effect would be more pronounced. The variation in intensity of MP band could also be explained in terms of phonon−plasmon coupling due to high local density of anisotropic carriers in CuO nanostructures. The change in peak position of MP band may be induced by the electronic density variation in the direction of the x^2-y^2 plane.

3.4. Transformation Mechanism of $Cu(OH)_2$ to CuO Nanostructures. Copper hydroxide $Cu(OH)_2$ is a metastable phase which easily transforms into more stable copper oxide, CuO.[52−56] This transformation occurs in solid state by thermal dehydration at a relatively low temperature, but exists also in aqueous media at room temperature. Copper hydroxide was easily decomposed thermally or by electron irradiation in an electronic microscope. Thermal decomposition of $Cu(OH)_2$ in the range of 298−1273 K in air was followed by means of a high-temperature X-ray powder diffraction camera. In order to understand the transformation from a crystallographical point of view, it is necessary briefly to describe the crystal structure of the two solids. The crystal structure of copper(II) hydroxide is orthorhombic, space group $Cmc2_1$ (No. 36) with $a = 2.9471$ Å, $b = 10.593$ Å, $c = 5.256\,44$ Å, $Z = 4$.[57] It is related to lepidocrocite γ-FeO(OH).[55] The structure presents corrugated layers perpendicular to the b-axis, in which copper(II) has a pentahedral surrounding composed of five OH^- ions (Cu−O: 1.95, 1.95, 1.97, 1.97, and 2.36 Å).The structure of CuO is monoclinic, space group $C2/c$ (No. 15): $a = 4.6837$ Å, $b = 3.4226$ Å, $c = 5.1288$ Å, $\beta = 99.54°$, $Z = 4$. It is built of crossing bands of copper(II) with square planar entities CuO_4, linked together by two opposite edges and spreading out in the directions [110] and $[\bar{1}11]$.[57] In all crystallized solids, divalent copper surroundings are always very distorted by a strong Jahn−Teller effect which often leads to square planar groups that are more stable. It has been reported that[53,54] the pure copper hydroxide can stay several months in pure water at room temperature without being transformed in CuO. Nevertheless, a slow transformation is thermodynamically possible because the solubility found in pure water is more important for $Cu(OH)_2$ (1.3×10^{-5} mol L^{-1}) than for CuO (2×10^{-7} mol L^{-1}).[53] It is quite different in the presence of hydroxide ions OH^-. Kinetics of transformation is very fast for the reason that divalent copper ions are dissolved under the form of tetrahydroxocuprate(II) anions $Cu(OH)_4^{2-}$. Concentrations of divalent copper in soda solutions are found around 10^{-3} mol L^{-1} and can reach 6×10^{-2} mol L^{-1} in very concentrated soda solutions. It is clear that copper concentrations can present such values only if copper is involved in a complex anion like $Cu(OH)_4^{2-}$, stabilized by the strong Jahn−Teller effect displayed by divalent copper, which leads to a square planar surrounding. This anion can be considered as a precursor entity for the formation of CuO. In fact, a condensation phenomenon, combined with a loss of two hydroxyl ions and one water molecule, leads to the formation of chains of square planar CuO_4 groups and then to solid CuO. Consequently, we think that the transformation of $Cu(OH)_2$ into more stable CuO, in aqueous solution at room temperature, is a reconstructive transformation involving a dissolution reaction followed by the precipitation of CuO,[54] according to the following scheme:

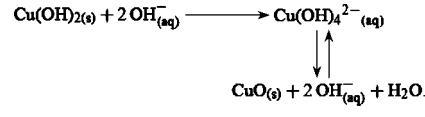

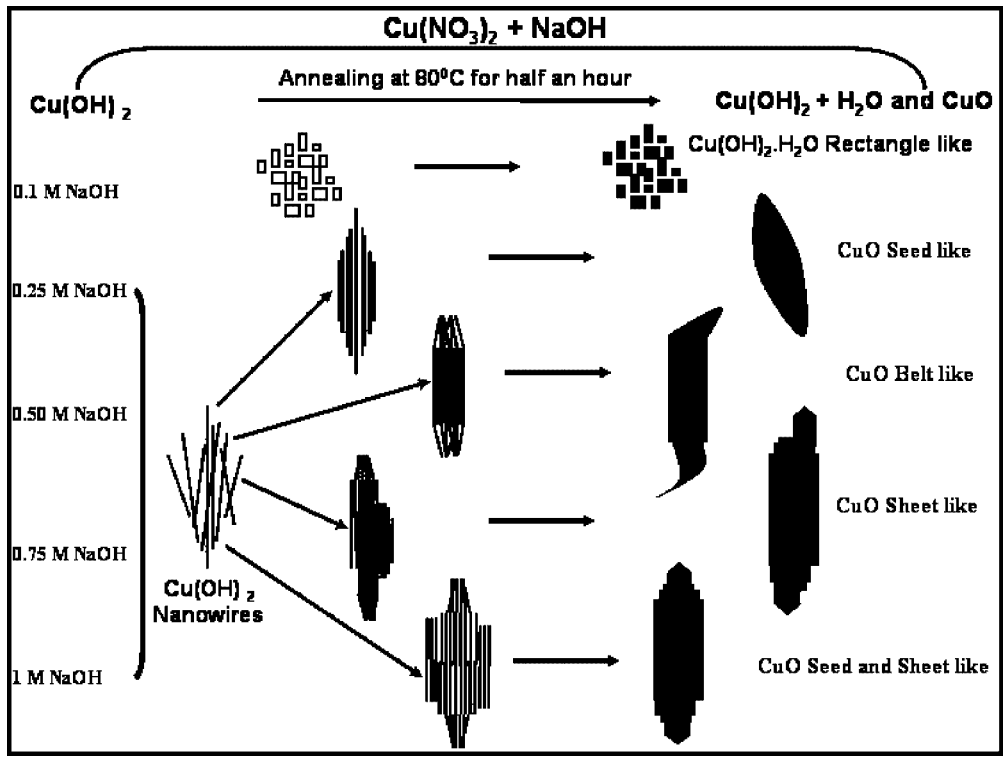

Figure 10. Schematic illustration of the growth of different $Cu(OH)_2$ and CuO nanoarchitectures under different conditions.

This transformation of $Cu(OH)_2$ into CuO is very fast at room temperature in soda solutions. Even if copper hydroxide decomposes at room temperature in aqueous soda solutions by a reconstructive transformation, a structural relationship exists with CuO. At a higher temperature it is evident that a topotactic or pseudomorphic transformation takes place within the solid phase. Nevertheless, the main feature common to the two different routes, performed either in solution or in the solid state, is the formation of square planar entities CuO4, which can be considered as the elementary bricks, giving rise to CuO.

3.5. Discussion. Addition of sodium hydroxide solution to copper nitrate solution produced a light blue or blue color precipitate of copper hydroxide.

$$Cu(NO_3)_2 + 2NaOH \rightarrow Cu(OH)_2 + 2NaNO_3$$

$$Cu(OH)_2 \rightarrow CuO + H_2O$$

To realize the controlled synthesis of assembled nanoarchitectures, many recent efforts have been directed to the morphological and structural control of primary building blocks. Many experimental parameters, such as reaction temperature, reactant concentration, and surfactant, can be manipulated to control the morphology and microstructure of nanocrystals. In addition, the pH value also has a significant influence on the morphology and dimensionality control. In the present work, our main concept is focused on the dimensionality control of CuO primary crystals by changing the solution pH value, thus modulating the morphology and dimensionality of the final assembled nanostructures. As is well-known, pH-tunable nanostructures have been extensively studied before; especially the aspect ratio of low-dimensional nanostructures is thought to be easily adjusted by changing the pH value. This is on the basis of the fact that the concentration of OH^- can significantly affect the nucleation and growth behaviors (such as the number of nuclei and the concentration of "growth units") of the nanocrystals.

3.6. Schematic Illustration for the Formation of Different $Cu(OH)_2$ and CuO Nanostructures. A schematic illustration for the growth of different $Cu(OH)_2$ and CuO nanoarchitectures under different conditions is shown in Figure 10. As soon as we mix the NaOH solution with the $Cu(NO_3)_2$ solution, $Cu(OH)_2$ material is formed instantly. TEM and SEM study revealed that these were either rectangle shaped nanoparticles or nanowires of $Cu(OH)_2$. As can be seen from the TEM micrographs of Figure 2, at concentration of 0.1 M the nanoparticles were of rectangle shape, whereas at the concentration of 0.25, 0.50, 0.75, and 1 M nanowire-like structures were formed. Due to their strong interacting nature, these nanowires instantly assembled in typical manner and resulted in different nanostructures of $Cu(OH)_2$ at the respective concentrations. TEM micrographs of the as-prepared $Cu(OH)_2$ nanowires revealed that they have a greater tendency to form bundles rather than in isolated randomly oriented $Cu(OH)_2$ nanowires. Annealing of as-obtained $Cu(OH)_2$ materials at 80 °C for half an hour resulted in hydrated $Cu(OH)_2$ and CuO nanostructures. From the XRD pattern (Figure 3), it can be seen that there is a complete transformation of $Cu(OH)_2$ nanowires into different nanostructures of CuO. It is important to mention here that at the concentration of 0.25, 0.50, 0.75, and 1 M NaOH the nanowire-like structures of $Cu(OH)_2$ were instantly formed. These nanowires by assembling parallel to their length resulted in the different nanostructures of $Cu(OH)_2$ which can be clearly seen in the TEM micrographs of Figure 2. As we anneal the material the $Cu(OH)_2$ gets transformed into the corresponding shape and size nanostructures of CuO but with better crystallinity.

Furthermore, high basic condition and appropriate volume ratio of $Cu(NO_3)_2$/NaOH are crucial in the formation of CuO nanostructures. We have varied the molar concentration of NaOH solution from 0.1 to 1 M keeping the volume ratio constant at ~50 mL of both solutions. As we increase the molar concentration of NaOH and hence the OH ion concentration,

the reaction kinetics and growth of the nanostructures took place in different ways. The faster and slower reaction kinetics are responsible for the formation of different nanostructures.

It has been observed that high ionic strength conditions are also responsible for the transformation of nanostructures. Xu et al.[58] have investigated the salt-mediated formation of free-standing Co_3O_4 nanocubes at 95 °C. They have seen the subsequent oxidation conversion of Co_3O_4 under high ionic strength conditions (by adding $NaNO_3$ salt in synthesis) at 95 °C. With the mediation of $NaNO_3$ salt in synthesis, formation of perfectly faceted Co_3O_4 nanocubes can be attributed to a lowering in O_2 solubility and creation of salt−(solvent)*n* diffusion boundary on the surfaces, which retards the cobalt oxidation and alters the normal interfacial growth under nonsalted conditions. In our case, salt $NaNO_3$ is automatically formed by the reaction of $Cu(NO_3)_2$ and NaOH solution. By varying the molar concentration of NaOH, we vary the salt concentration of NaOH in the media. We believe that the salt concentration of $NaNO_3$ in the medium is also responsible for the faster and slower reaction kinetics and hence the transformation of $Cu(OH)_2$ to CuO nanostructures.

4. Conclusions

1. Different copper hydroxide $Cu(OH)_2$ and copper oxide (CuO) (nanowires, and rectangle-, seed-, belt-, and sheetlike) nanostructures have been synthesized by wet chemical method. This method consists of simple addition of copper nitrate solution to the sodium hydroxide solution in 1:1 ratio.

2. Different copper oxide (CuO) (rectangle-like, seedlike, beltlike, and sheetlike) nanostructures have been synthesized by addition of different molar concentration of NaOH solution (0.1, 0.25, 0.50, and 1 M, respectively) to the copper nitrate solution (0.2 M), followed by heating the solution at 80 °C for half an hour.

3. A tentative mechanism has been given for the formation and transformation of the nanostructures. Various experiments and their structural/microstructural investigations revealed that at first various $Cu(OH)_2$ nanostructures are formed which get transformed into corresponding shape and size nanostructures of CuO after annealing at 80 °C for half an hour.

Acknowledgment. The authors are extremely grateful to Dr. N. N. Rao, NERI, Nagpur, and Prof. A. Roy, IITKH, India, for their help, encouragement, and fruitful discussions. The authors acknowledge with gratitude the financial support from DST, UNANST, Council of Scientific and Industrial Research (CSIR), Ministry of New and Renewable Energy (MNRE), and University Grant Commission (UGC) New Delhi, India.

References and Notes

(1) Cui, Y.; Wei, Q. Q.; Park, H. K.; Liber, C. M. *Science* **2001**, *293*, 1289.
(2) Favier, F.; Walter, E. C.; Zach, M. P.; Benter, T.; Penner, R. M. *Science* **2001**, *293*, 2227.
(3) Huang, M. H.; Mao, S.; Fe'ck, H.; Yen, H. Q.; Wu, Y. Y.; Kind, H.; Waber, E.; Russo, R.; Yang, P. D. *Science* **2001**, *292*, 1897.
(4) Lauhon, L. J.; Gudiksen, M. S.; Wang, D. L.; Lieber, C. M. *Nature* **2002**, *420*, 57.
(5) Meunier, B. *Chem. Rev.* **1992**, *92*, 1411.
(6) Schweigert, N.; Acero, J.; Von Gunten, U.; Canonica, S.; Zehnder, A.; Eggen, R.; Environ, *Mol. Mutagen* **2000**, *36*, 5.
(7) Pote, J. E.; Cruse, R. W.; Karlin, K. D.; Solomon, E. I. *J. Am. Chem. Soc.* **1987**, *109*, 2624.
(8) Pote, J. E.; Ross, P. K.; Thamann, Th. J.; Reed, C. A.; Karlin, K. D.; Surrell, Th, N.; Solomon, E. I. *J. Am. Chem. Soc.* **1989**, *111*, 5198.
(9) Fujita, W.; Awaga, K. *Synth. Met.* **2001**, *122*, 569.
(10) Fujita, W.; Awaga, K. *Inorg. Chem.* **1996**, *35*, 1915.
(11) Fujita, W.; Awaga, K. *J. Am. Chem. Soc.* **1997**, 45633.
(12) Wang, W. Z.; Wang, G. H.; Wang, X. S.; Zhan, R. J.; Liu, Y. K.; Zheng, C. L. *Adv. Mater.* **2002**, *14*, 67.
(13) Durand-Keklikian, L.; Matijevic, E. *Colloid Polym. Sci.* **1990**, *268*, 1151.
(14) Kratohuil, S.; Matijevic, E. *J. Mater. Res.* **1991**, *6*, 766.
(15) Rodriguez-Clemente, R.; Serna, C. J.; Ocana, M.; Matijevic, E. *J. Cryst. Growth* **1994**, *143*, 277.
(16) Wen, X.; Zhang, W.; Yang, S.; Dai, Z. R.; Wang, Z. L. *Nano Lett.* **2002**, *2*, 1397.
(17) Wen, X.; Zhang, W.; Yang, S. *Langmuir* **2003**, *19*, 5898.
(18) Park, S. H.; Kim, H. J. *J. Am. Chem. Soc.* **2004**, *126*, 14368.
(19) Wang, W.; Lan, C.; Li, Y.; Hong, K.; Wang, G. *Chem. Phys. Lett.* **2002**, *366*, 220.
(20) Lu, C.; Qi, L.; Yang, J.; Zhang, D. J.; Wu, N.; Ma, J. *J. Phys. Chem. B* **2004**, *108*, 17825.
(21) Song, X.; Sun, S.; Zhang, W.; Yu, H.; Fan, W. *J. Phys. Chem. B* **2004**, *108*, 5200.
(22) Luo, Y. H.; Huang, J.; Jin, J.; Peng, X.; Schmitt, W.; Ichinose, I. *Chem. Mater.* **2006**, *18*, 1795.
(23) Zheng, X. G.; Xu, C. N.; Tomokiyo, Y.; Tanaka, E.; Yamada, H.; Soejima, Y. *Phys. Rev. Lett.* **2000**, *85*, 5170.
(24) Borgohain, K.; Mahamuni, S. *J. Mater. Res.* **2002**, *17*, 1220.
(25) Maruyama, T. *Sol. Energy Mater. Sol. Cells* **1998**, *56*, 85.
(26) Rakhshani, A. E. *Solid-State Electron.* **1986**, *29*, 7.
(27) Lanza, F.; Feduzi, R.; Fuger, J. *J. Mater. Res.* **1990**, *5*, 1739.
(28) Gao, X. P.; Bao, J. L.; Pon, G. L.; Zhu, H. Y.; Huang, P. X.; Wu, F.; Song, D. Y. *J. Phys. Chem. B* **2004**, *108*, 5547.
(29) Reitz, J. B.; Solomon, E. I. *J. Am. Chem. Soc.* **1998**, *120*, 11467.
(30) Frietsch, M.; Zudock, F.; Goschnick, J.; Bruns, M. *Sensors Actuators, B* **2000**, *65*, 379.
(31) Dai, P. C.; Mook, H. A.; Appli, G.; Hayden, S. M.; Dogan, F. *Nature* **2000**, *406*, 965.
(32) Deng, J. F.; Sun, Q.; Zhang, Y. L.; Chen, S. Y.; Wu, D. *Appl. Catal. A* **1996**, *139*, 75.
(33) Terakura, K.; Oguchi, T.; Williams, A. R.; Kubler, J. *Phys. Rev. B* **1984**, *30*, 4734.
(34) Norman, M. R.; Freeman, A. J. *Phys. Rev. B* **1986**, *33*, 8896.
(35) Yang, B. X.; Thurston, T. R.; Tranquada, J. M.; Shiranc, G. *Phys. Rev. B* **1989**, *39*, 4343.
(36) Sukhorukov, Y. P.; Loshkareva, N. N.; Samokhvalov, A. A.; Naumov, S. V.; Moskvin, A. S.; Ouchinnikov, A. S. *J. Magn. Magn. Mater.* **1998**, *183*, 356.
(37) (a) Lee, S. H.; Her, Y. S.; Matijevic, E. *J. Colloid Interface Sci.* **1997**, *186*, 193. (b) Liangy, Z. H.; Zhu, Y. J. *Chem. Lett.* **2004**, *33*, 1314. (c) Yang, R.; Gao, L. *Chem. Lett.* **2004**, *33*, 1194.
(38) (a) Cao, M. H.; Hu, C. W.; Wang, Y. H.; Guo, Y. H.; Guo, C. X.; Wang, E. B. *Chem. Commun.* **2003**, 1884. (b) Jiang, X. C.; Herricks, T.; Xia, Y. N. *Nano Lett.* **2002**, *2*, 1333. (c) Du, G. H.; Van Tendeloo, G. *Chem. Phys. Lett.* **2004**, *393*, 64. (d) Wang, W. Z.; Varghese, O. K.; Ruan, C. M.; Paulose, M.; Grimes, C. A. *J. Mater. Res.* **2003**, *18*, 2756.
(39) (a) Chang, Y.; Zeng, H. C. *Cryst. Growth Des.* **2004**, *4*, 397. (b) Lu, C. H.; Qi, L. M.; Yang, J. H.; Zhang, D. Y.; Wu, N. Z.; Ma, J. M. *J. Phys. Chem. B* **2004**, *108*, 17825. (c) Gao, X. P.; Bao, J. L.; Pan, G. L.; Zhu, H. Y.; Huang, P. X.; Wu, F.; Song, D. Y. *J. Phys. Chem.B* **2004**, *108*, 5547.
(40) (a) Hou, H. W.; Xie, Y.; Li, Q. *Cryst. Growth Des.* **2005**, *5*, 201. (b) Fan, H. M.; Yang, L. T.; Hua, W. S.; Wu, X. F.; Wu, Z. Y.; Xie, S. S.; Zuo, B. S. *Nanotechnology* **2004**, *15*, 37. (c) Zhu, J. W.; Chen, H. Q.; Liu, H. B.; Yang, X. J.; Lu, L. D.; Wang, X. *Mater. Sci. Eng., A* **2004**, *384*, 172.
(41) (a) Zhao, Y.; Zhu, J. J.; Hong, J. M.; Bian, N. S.; Chen, H. Y. *Eur. J. Inorg. Chem.* **2004**, 4072. (b) Yu, T.; Cheong, F. C.; Sow, C. H. *Nanotechnology* **2004**, *15*, 1732. (c) Zhu, Y. W.; Yu, T.; Cheong, F. C.; Xu, X. J.; Lim, C. T.; Tan, V. B. C.; Thong, J. T. L.; Sow, C. H. *Nanotechnology* **2005**, *16*, 88.
(42) (a) Zhu, C. L.; Chen, C. N.; Hao, L. Y.; Hu, Y.; Chen, Z. Y. *Solid State Commun.* **2004**, *130*, 681. (b) Li, D.; Leung, Y. H.; Djurisic, A. B.; Liu, Z. T.; Xie, M. H.; Gao, J.; Chan, W. K. *J. Cryst. Growth* **2005**, *282*, 105. (c) Chen, D.; Shen, G. Z.; Tang, K. B.; Qian, Y. T. *J. Cryst. Growth* **2003**, *254*, 225.
(43) (a) Yao, W. T.; Yu, S. H.; Zhou, Y.; Jiang, J.; Wu, Q. S.; Zhang, L.; Jiang, J. *J. Phys. Chem. B* **2005**, *109*, 14011. (b) Song, X. Y.; Sun, S. X.; Zhang, W. M.; Yu, H. Y.; Fan, W. L. *J. Phys. Chem. B* **2004**, *108*, 5200. (c) Wu, X. F.; Bai, H.; Zhang, J. X.; Chen, F. E.; Shi, G. Q. *J. Phys. Chem. B* **2005**, *109*, 22836. (d) Xu, C. K.; Liu, Y. K.; Xu, G. D.; Wang, G. G. *Mater. Res. Bull.* **2002**, *37*, 2365.
(44) (a) Zhang, W. X.; Wen, X. G.; Yang, S. H.; Berta, Y.; Wang, Z. L. *AdV. Mater.* **2003**, *15*, 822. (b) Kumar, R. V.; Diamant, Y.; Gedanken, A. *Chem. Mater.* **2000**, *12*, 2301. (c) Wen, X. G.; Zhang, W. X.; Yang, S. H. *Langmuir* **2003**, *19*, 5898. (d) Zhang, W. X.; Wen, X. G.; Yang, S. H. *Inorg. Chem.* **2003**, *42*, 5005. (e) Wen, X. G.; Zhang, W. X.; Yang, S. H.; Dai, Z. R.; Wang, Z. L. *Nano Lett.* **2002**, *2*, 1397.

(45) Zhang, L. Z.; Yu, J. C.; Xu, A. W.; Li, Q.; Kwong, K. W.; Yu, S. H. *J. Cryst. Growth* **2004**, *266*, 545.
(46) Xu, Y. Y.; Chen, D. R.; Jiao, X. L. *J. Phys. Chem. B* **2005**, *109*, 13561.
(47) Xu, J. S.; Xue, D. F. *J. Phys. Chem. B* **2005**, *109*, 17157.
(48) Li, S. Z.; Zhang, H.; Ji, Y. J.; Yang, D. R. *Nanotechnology* **2004**, *15*, 1428.
(49) Zhang, Z. P.; Sun, H. P.; Shao, X. Q.; Li, D. F.; Yu, H. D.; Han, M. Y. *Adv. Mater.* **2005**, *17*, 42.
(50) Liu, B.; Zeng, H. C. *J. Am. Chem. Soc.* **2004**, *126*, 8124.
(51) Liu, Y.; Chu, Y.; Li, M. Y.; Dong, L. H. *J.Mater. Chem.* **2006**, *16*, 192.
(52) Cudennec, Y.; Lecerf, A.; Riou, A.; Gérault, Y. *Eur. J. Solid State Inorg. Chem.* **1988**, *25*, 351.
(53) Cudennec, Y.; Lecerf, A.; Gérault, Y. *Eur. J. Solid State Inorg. Chem.* **1995**, *32*, 1013.
(54) Cudennec, Y.; Riou, A.; Lecerf, A.; Gérault, Y. C. R. *Acad. Sci. Paris, Ser. IIc* **2000**, *3*, 661.
(55) Cudennec, Y.; Lecerf, A. C. R. *Acad. Sci. Paris, Chem.* **2001**, *4*, 885.
(56) Günter, J. R.; Ostwald, H. R. *J. Appl. Crystallogr.* **1970**, *3*, 21.
(57) Cudennec, Y.; Lecerf, A. *Solid State Sci.* **2003**, *5*, 1471.
(58) Xu, R.; Zeng, H. C. *J. Phys. Chem. B* **2003**, *107*, 926.

JP804832G